Talanta 103 (2013) 361–370

Contents lists available at SciVerse ScienceDirect

Talanta

journal homepage: www.elsevier.com/locate/talanta

Feasibility of the determination of polycyclic aromatic hydrocarbons in edible oils *via* unfolded partial least-squares/residual bilinearization and parallel factor analysis of fluorescence excitation emission matrices

Francis Alarcón [a], María E. Báez [a], Manuel Bravo [b], Pablo Richter [a], Graciela M. Escandar [c], Alejandro C. Olivieri [c], Edwar Fuentes [a,*]

[a] Departamento de Química Inorgánica y Analítica, Facultad de Ciencias Químicas y Farmacéuticas, Universidad de Chile, Santiago, Casilla 233, Chile
[b] Laboratorio de Química Analítica y Ambiental, Instituto de Química, Facultad de Ciencias, Pontificia Universidad Católica de Valparaíso, Avenida Brasil 2950, Valparaíso, Chile
[c] Instituto de Química Rosario (IQUIR-CONICET-UNR), Facultad de Ciencias Bioquímicas y Farmacéuticas, Universidad Nacional de Rosario, Suipacha 531 (2000), Rosario, Argentina

ARTICLE INFO

Article history:
Received 31 August 2012
Received in revised form
23 October 2012
Accepted 25 October 2012
Available online 2 November 2012

Keywords:
Polycyclic aromatic hydrocarbons
Edible oils
Fluorescence excitation–emission matrices
Multivariate calibration

ABSTRACT

The possibility of simultaneously determining seven concerned heavy polycyclic aromatic hydrocarbons (PAHs) of the US-EPA priority pollutant list, in extra virgin olive and sunflower oils was examined using unfolded partial least-squares with residual bilinearization (U-PLS/RBL) and parallel factor analysis (PARAFAC). Both of these methods were applied to fluorescence excitation emission matrices. The compounds studied were benzo[*a*]anthracene, benzo[*b*]fluoranthene, benzo[*k*]fluoranthene, benzo[*a*]pyrene, dibenz[*a*,*h*]anthracene, benzo[*g*,*h*,*i*]perylene and indeno[1,2,3-*c*,*d*]-pyrene. The analysis was performed using fluorescence spectroscopy after a microwave assisted liquid–liquid extraction and solid-phase extraction on silica. The U-PLS/RBL algorithm exhibited the best performance for resolving the heavy PAH mixture in the presence of both the highly complex oil matrix and other unpredicted PAHs of the US-EPA list. The obtained limit of detection for the proposed method ranged from 0.07 to 2 μg kg^{-1}. The predicted U-PLS/RBL concentrations were satisfactorily compared with those obtained using high-performance liquid chromatography with fluorescence detection. A simple analysis with a considerable reduction in time and solvent consumption in comparison with chromatography are the principal advantages of the proposed method.

1. Introduction

Polycyclic aromatic hydrocarbons (PAHs) constitute a large family of organic compounds that contain two or more fused aromatic rings that are composed of carbon and hydrogen atoms [1]. PAHs are of interest primarily because of their carcinogenic and mutagenic characteristics, especially those of high molecular weight (5–6 fused aromatic rings). These compounds are primarily formed by the incomplete combustion of organic matter and are continuously released into the atmosphere from natural and anthropogenic sources [2–4].

Humans are primarily exposed to PAHs through the direct inhalation of polluted air or tobacco smoke, direct contact by skin with polluted soils, soot or tars and intake of contaminated water or foods, especially fatty food (animal or vegetable) [5]. According to Diletti et al., one of the most important sources of exposure to PAHs for non-smoking humans is food contaminated from air, soil and water and during processing and cooking [6], whereas Barranco et al. proposed that the human intake of PAHs from food is considerably greater than that from air or drinking water, and edible oils and fats are the major source [7].

The occurrence of PAHs in edible oils is primarily attributed to environmental contamination of raw vegetable materials and to contamination from some operations conducted during their processing, in which processes such as seed drying, solvent extraction, soil burning, packaging of materials and mineral oils used to lubricated the machinery for extracting oil from plants represent possible contamination sources [4,8–10].

The carcinogenic and mutagenic characteristics of the heavier PAHs of the United States EPA (Environmental Protection Agency) priority pollutant list justify the careful analytical control of their presence in foods, specifically fatty foods, and make the development of clear cut and uniform legislations necessary. In July 2001, Spain passed a legislation that limits the concentration of eight heavy PAHs in olive pomace oils, including benz[*a*]anthracene (BaA), benzo[*b*]fluoranthene (BbF), benzo[*k*]fluoranthene (BkF), benzo[*e*]pyrene (BeP), benzo[*a*]pyrene (BaP), indeno[1,2,3-*c*,*d*]-pyrene (IP), dibenz[*a*,*h*]anthracene (DBahA) and benzo[*g*,*h*,*i*]perylene

* Corresponding author. Tel.: +56 2 9782830.
E-mail address: edfuentes@ciq.uchile.cl (E. Fuentes).

0039-9140/$ - see front matter © 2012 Elsevier B.V. All rights reserved.
http://dx.doi.org/10.1016/j.talanta.2012.10.080

(BghiP). A maximum limit of 2 μg kg^{-1} for each single PAH and 5 μg kg^{-1} for the sum of the eight heavy PAHs was established [8,10–12]. In 2003, Chile modified its Sanitary Decree N° 977 of 1996 and established the same maximum limits as the Spanish legislation for edible oils and fats in general [13].

The two major problems associated with the determination of PAHs in complex matrices, such as vegetable oils and fats, are the diversity of potential interferences and the low analyte levels [9]. The majority of the methods for the determination of PAHs generally involve an extraction step, followed by clean-up and, finally, a chromatographic determination. All of these methodologies are laborious, time-consuming and expensive, not only for the sample pretreatment but also for the analytical determination. One alternative to chromatographic analysis is fluorescence spectroscopy. Molecular fluorescence measurements can be rapidly and inexpensively performed. Many environmentally important hydrocarbon contaminants are naturally fluorescent and detectable at μg kg^{-1} level. Unfortunately, the broad fluorescence bands and the considerable number of naturally fluorescent compounds prevent complete analyte selectivity with both excitation- and emission-based measurements [14,15]. A modern approach to improve the selectivity of this analytical method is the use of advanced chemometric tools, such as second-order multivariate calibration methods. Some second-order methods allow for direct determination of concentrations and estimations of spectral profiles of sample components. This property, which is named the second-order advantage, avoids the physical removal of interferences or the construction of large and diverse calibration sets [15–19].

Recently some authors have proposed the use of high resolution luminescence (Shpol'skii spectroscopy) for the direct determination of US-EPA-PAHs without chromatographic separation in soil [20] and water samples [21] and heavy-molecular weight PAHs (molecular weight 302 g mol^{-1}) in water samples [22].

The present work explores the possibility of applying the total fluorescence spectroscopy technique, combined with the second-order multivariate calibration methods, for the simultaneous determination of seven heavy PAHs of the US-EPA list in edible oils, including BaA, BbF, BkF, BaP, DBahA, BghiP and IP. Microwave-assisted liquid–liquid extraction coupled to solid phase extraction with silica was required as a previous sample preparation step. The selected second-order calibration methods were unfolded partial least-squares coupled to residual bilinearization (U-PLS/RBL) and parallel factor analysis (PARAFAC). In addition, some analyses were performed in the presence of nine of the remaining priority US-EPA PAHs as additional potential interferences. Remarkable differences in the prediction capabilities of the employed algorithms are shown and discussed. Finally, the feasibility of determining the seven selected PAHs in samples of edible oils is demonstrated.

2. Theory

2.1. Parallel factor analysis (PARAFAC)

Excitation–emission fluorescence measurements can provide a three-way data set, in which each sample provides an excitation–emission fluorescence data matrix (EEFM). A series of data matrices obtained for multiple samples compose a three-way array, **X**. The PARAFAC algorithm decomposes the data array **X** and generates a trilinear model that minimizes the sum of the squares of the residuals (e_{ijk}), as indicated in Eq. (1),

$$x_{ijk} = \sum_{f=1}^{F} a_{if} b_{jf} c_{kf} + e_{ijk} \quad (1)$$

where the element x_{ijk} of **X** represents the datum for sample i at the instrumental channels j and k (e.g., the excitation and emission wavelengths). The three-way data array is decomposed into a set of sample scores, a_{if}, loadings for the emission mode, b_{jf}, and loadings for the excitation mode, c_{kf}. The rank of the PARAFAC model is given by the number of factors, F, that are required to describe the systematic variation in the data array. A crucial stage in the development of the model is the determination of F [23–25]. There are various criteria for evaluating F, including the percentage of fit and the core consistency test [24,26], which provide a measure of the variability of the experimental data reflected by the model. Values close to one hundred in both parameters are desirable.

The decomposition of the three-way data usually provides a unique mathematical solution for a given number of components. Therefore, there are no mathematical ambiguities in the solution, except for trivial scale and order issues. Therefore, if the PARAFAC model is also a description of the chemically meaningful structure, the parameters of the model will have a chemical interpretation. Specifically, each PARAFAC component will be an estimate of the contribution from one fluorophore, and this estimate is provided by a score vector that contains the relative concentrations, an emission loading that is an estimate of the emission spectrum and an excitation loading that is an estimate of the excitation spectrum. Therefore, the PARAFAC model can be used for a unique decomposition of the fluorescence data from a complex sample set into a number of PARAFAC components that correspond to the number of fluorophores present in the samples [23]. To evaluate the quality of the retrieved profiles, we used the criterion of similarity (correlation coefficient, r) and compared the true spectra with the spectra obtained using the PARAFAC algorithm. A value of $r=1$ indicates total coincidence.

2.2. Unfolded partial least squares with residual bilinearization (U-PLS/RBL)

The U-PLS method is a variant of the classical partial least squares (PLS) that was proposed for second-order data where three-way data are unfolded into vectors before two-way PLS calibration [27]. If the calibration was exact, the regression coefficients, $\boldsymbol{v}$, could be employed to estimate the analyte concentrations in an unknown specimen using Eq. (2),

$$y_u = \boldsymbol{t_u^T v} \quad (2)$$

where t_u is the test sample score, which is obtained by projection of the (unfolded) data for the test sample X_u onto the space of the A latent factors, as indicated in Eq. (3).

$$t_u = \left(W^T P\right)^{-1} W^T \mathrm{vec}(X_u) \quad (3)$$

However, the U-PLS method must be coupled to RBL to achieve the second-order advantage. RBL is a post-calibration procedure that is based on principal component analysis (PCA) to model the presence of unexpected constituents in a sample [18,28–30]. The matrix data, X_u, for a sample with unexpected constituents is first vectorized [vec(X_u)] and then expressed as shown in Eq. (4).

$$\mathrm{vec}(X_u) = P t_u + [\mathbf{B}_{\mathrm{unx}} \mathbf{G}_{\mathrm{unx}} (\mathbf{C}_{\mathrm{unx}})^T] + \mathbf{e}_{\mathrm{RBL}} \quad (4)$$

where $\mathbf{e}_{\mathrm{RBL}}$ is the residual error RBL term and $\boldsymbol{B}_{\mathbf{unx}}$, $\boldsymbol{G}_{\mathbf{unx}}$, and $\boldsymbol{C}_{\mathbf{unx}}$ are provided by PCA [which is generally performed by singular value decomposition (SVD)] of a residual matrix, obtained after reshaping the computed residual vector $\mathbf{e}_{\mathrm{RBL}}$ and assuming that interferences are absent, as indicated in Eq. (5).

$$\boldsymbol{B}_{\mathbf{unx}} \boldsymbol{G}_{\mathbf{unx}} (\boldsymbol{C}_{\mathbf{unx}})^T = \mathrm{SVD}\{\mathrm{reshape}[\mathrm{vec}(X_u) - P t_u]\} \quad (5)$$

here, "reshape" indicates the reverse operation of the vectorization, i.e., conversion of a $JK \times 1$ vector into a $J \times K$ matrix, and the SVD operation is performed using the first N_{unx} principal components, where N_{unx} indicates the number of unexpected test sample constituents.

The RBL procedure consists maintaining the matrix of loadings P in Eq. (4) constant at the calibration values and varying t_u in this latter equation to minimize the norm of $\boldsymbol{e}_{RBL}$ ($|\boldsymbol{e}_{RBL}|$). During the RBL minimization, profiles for the unexpected constituents are continually updated through Eq. (5). The standard deviation (s_{RBL}) of the residuals in Eq. (4) can be used as a measure of the goodness of fit (GOF) for the RBL procedure and, according to Bortolato et al., is given by Eq. (6) [18].

$$s_{RBL} = \|e_{RBL}\| / [(J - N_{unx})(K - N_{unx}) - A]^{1/2} \quad (6)$$

The number of unexpected constituents is usually estimated by inspecting the behavior of s_{RBL} with increasing values of N_{unx}. The s_{RBL} is assumed to stabilize at a value compatible with the instrumental noise when the correct value of N_{unx} is reached. However, when the number of unexpected constituents is large, as in the present case, the latter method does not provide reliable results. This result is consistent with the fact that model selection guided by the GOF generally underestimates the generalization error of a model. An interesting alternative procedure for estimating N_{unx} is to apply the so-called generalized cross-validation (GCV) criterion, which can be adapted to the present case by first defining a penalized residual error (s_{pen}), which is calculated in a manner analogous to the GCV error:

$$s_{pen} = s_{RBL}[(J \times K)/[(J - N_{unx})(K - N_{unx}) - A]^{1/2}] \quad (7)$$

To estimate the optimum number of unexpected constituents for RBL, the following ratio was computed for increasing values of N_{unx}:

$$R = s_{pen}(N_{unx})/[s_{RBL}(N_{unx} - 1)] \quad (8)$$

The first value of N_{unx} where R did not exceed 1 was then selected as the number of RBL components. This process is one of the recommended procedures for comparing cross-validation with auto-prediction residuals errors [18].

3. Experimental

3.1. Reagents and solutions

Acenaphthylene (ACEN), anthracene (AN), phenanthrene (PHEN), fluoranthene (FLT), fluorene (FLU), benzo[*b*]fluoranthene (BbF), benzo[*k*]fluoranthene (BkF) and indeno[1,2,3-*c*,*d*]-pyrene (IP) were purchased from Accustandard (New Haven, CT, USA); acenaphthene (AC), pyrene (PYR) and chrysene (CHR) were obtained from Supelco (Bellefonte, PA, USA); naphthalene (NAPH), benz[*a*]anthracene (BaA) and benzo[*g*,*h*,*i*]perylene (BghiP) were purchased from Aldrich (Steinheim, Germany); and benzo[*a*]pyrene (BaP) and dibenz[*a*,*h*]anthracene (DBahA) were obtained from Dr. Ehrenstorfer (Augsburg, Germany). All reagents were of high-purity grade and used as received.

Acetonitrile, *n*-hexane and 2-propanol were purchased form Merck (Darmstadt, Germany), and dichloromethane was obtained from Mallinckrodt Chemicals (Phillipsburg, PH, USA). All of these reagents were of HPLC grade and used as received.

Stock solutions of pure analytes (100 μg mL^{-1}) were prepared in acetonitrile. From these solutions, more diluted solutions (100 μg L^{-1}) in *n*-hexane were obtained in appropriate volumes, evaporating under a nitrogen stream and diluting with *n*-hexane. All of the solutions were stored in silaned amber vials at 4 °C in darkness. The solutions were stable for almost six months. The PAH reagents were handled with extreme caution, including the use of gloves and protective clothing.

3.2. Apparatus and software

A Milestone Microwave Laboratory System (Sorisole, BG, Italy) equipped with a high-performance microwave digestion unit model mls-1200 Mega, an exhaust module model EM-45/A, a terminal Mega-240 and a 10-position rotor was used for the sample preparation.

A Varian Cary-Eclipse luminescence spectrometer (Mulgrave, Australia) equipped with a xenon flash lamp was used to obtain the excitation–emission fluorescent measurements. Quartz cells with a 1.00 cm path length were used, and the EEFMs were recorded in the λ_{exc} ranges of 250–400 nm every 5 nm and λ_{em} of 370–550 nm every 2 nm. The widths of the excitation and emission slits were 10 nm. The spectra were saved in ASCII format and transferred to a computer for subsequent manipulation.

High-performance liquid chromatography with fluorescence detector (HPLC-FLD) analysis was performed on a liquid chromatograph equipped with a Waters 600 HPLC pump, a Waters 2475 fluorescence detector and a Waters 717 auto sampler (Milford, MA, USA). The column was an Intertsil HPLC ODS-P (250 × 4.6 mm ID, 5 μm particle size) purchased from GL Sciences (Tokyo, Japan). The mobile phase was a mixture of acetonitrile (A) and water (B) at a flow rate of 1.4 mL min^{-1}. The following gradient program was used: 0–0.1 min 70% A isocratic; 0.1–10 min linear gradient 90% A; 10–15 min 90% A isocratic; 15–20 min linear gradient 100% A; 20–32 min 100% A isocratic; and finally, back to the initial condition: 32–35 min linear gradient 70% A; 35–38 min 70% A isocratic. An injection volume of 20 μL was employed. Four channels were used to define the excitation and emission wavelengths ($\lambda_{exc}/\lambda_{em}$) in the fluorescence detector, as follows: channel A 220/330; channel B 292/410; channel C 292/426; and channel D 300/500.

The routines for data pre-treatment used to eliminate Rayleigh and Raman scattering peaks from the EEFMs [31] and subsequent data processing were implemented in MATLAB [32]. The routines employed for the PARAFAC and U-PLS/RBL are available on the internet [33]. All of the algorithms were implemented using the graphical interface of the MVC2 toolbox [34], which is also available on the internet [35].

3.3. Calibration set samples

A calibration set of 17 samples that contained the seven studied PAHs in *n*-hexane was prepared from the diluted solutions. Twelve samples of the set corresponded to the concentrations provided by a Plackett–Burman design. The tested concentrations were in the range of 0–2.00 μg L^{-1} for BaA, BbF, BaP and DBahA; 0–0.50 μg L^{-1} for BkF; 0–4.00 μg L^{-1} for BghiP; and 0–2.50 μg L^{-1} for IP. The remaining five samples corresponded to a blank solution, a solution that contained all of the studied PAHs at an average concentration (1.06 μg L^{-1} for BaA, BbF, BaP, DBahA and BghiP; 0.29 μg L^{-1} for BkF; and 1.50 μg L^{-1} for IP), a solution that contained BbF (2.00 μg L^{-1}) and two samples that contained BghiP at different concentrations (2.00 and 4.00 μg L^{-1}). The EFMMs were then read and subjected to second-order data analysis.

3.4. Validation set samples

Eleven samples of an organic extra-virgin olive oil (EVOO) purchased in a local supermarket were used to prepare the validation set. These samples were processed using the sample preparation procedure described below and spiked in the final

step with different volumes (order of μL) of diluted solutions of the seven selected PAHs. The EEFMs were then read and subjected to second-order data analysis. The validation sample set was prepared using the same concentration ranges as those used for the calibration set.

3.5. Test set samples

For testing the applicability of the investigated method, different brands and types of edible oils were analyzed. For this purpose, four brands of EVOO and two brands of common sunflower oil (SO) were purchased at a local supermarket. Because these samples did not contain PAHs or their concentrations were lower than the detection limits of the studied methods, a recovery and predictive capacity study was performed by spiking these samples with the seven studied PAHs at the beginning of the process with concentrations different that those used for calibration and following a random design. These samples were subsequently processed using the sample preparation procedure described below, and the EEFMs were read. A total of 25 spiked real samples were prepared for this purpose, including 17 samples from the four different brands of EVOO and 8 samples from the two brands of SO. These samples were also analyzed using HPLC-FLD as a reference method [1] (Table 3).

Additionally, to probe the predictive capacity of the models in presence of potentially interfering PAHs, another test set of four organic EVOO samples containing the remaining nine US-EPA-PAHs at a concentration of 3.00 μg kg^{-1} for each was prepared. The concentrations of the seven studied PAHs were as follows: 4.50 μg kg^{-1} for BaA, BbF, BaP and DBahA; 2.40 μg kg^{-1} for BkF; and 6.00 μg kg^{-1} for BghiP and IP. These latter sets of samples were also analyzed using HPLC-FLD.

3.6. Real samples

A set of twenty samples of edible oils (five brands of SO, one SO used to prepare fried fish and fourteen brands of EVOO) were analyzed using the proposed method and using HPLC-FLD.

3.7. Microwave-assisted liquid–liquid extraction coupled to solid phase extraction, MAE-SPE.

A glass system previously designed in our laboratory was used during the microwave-assisted extraction (MAE) [36]. An aliquot of 1.00 ± 0.01 g of oil was accurately weighed into a 50 mL Erlenmeyer flask equipped with a ground-glass joint. Then, 30 mL of acetonitrile was added, and an air-cooled condenser was attached to the ground-glass joint of the flask. The glass system was hated in a microwave oven for 19 min at 150 W. Only eight of the ten positions available in the rotor were used. After cooling, the inner wall of the condenser was rinsed with a few milliliters of acetonitrile and then removed from the flask. The top layer was carefully transferred with a Pasteur pipette into a 50 mL round-bottom flask, and the extract was concentrated to dryness in a vacuum rotary evaporator equipped with a 65 °C water bath. Then, the extract was dissolved in 1 mL of *n*-hexane.

The solid phase extraction clean-up was performed using a 2 g silica SPE cartridge obtained from Supelco (Bellefonte, PA, USA). The 2 g silica cartridge was previously washed with 5 mL of dichloromethane and conditioned with 5 mL of *n*-hexane. Then, 1 mL of the dissolved extract was loaded onto the cartridge (0.5 mL for SO oil), and the PAHs were eluted with a 15 mL mixture of *n*-hexane:dichloromethane 80:20 (v/v). All of the eluate was collected in a 22 mL amber vial and concentrated under a nitrogen stream. The residue was dissolved in 3 mL of *n*-hexane, and 2 mL was used to obtain the EEFMs in the luminescence spectrometer. The remaining volume was dried under a nitrogen stream and re-dissolved in 1 mL of 2-propanol for HPLC-FLD analysis.

4. Results and discussion

4.1. General considerations and sample treatment

Fig. 1A and B present the excitation and emission fluorescence spectra for the seven studied PAHs in *n*-hexane and the remaining nine US-EPA-PAHs, respectively. Different extents of overlapping clearly occur among the bands, and the situation becomes more significant if additional PAHs are present. Consequently, the simultaneous fluorimetric determination of PAHs represents a significant analytical challenge.

Additionally, in a previous work [37], we demonstrated that oil matrices complicate the determination of PAHs because of the presence of pigments (primarily pheophytin and chlorophyll) and tocopherols that produce inner filter phenomena and partial overlapping with the bands of PAHs at short wavelengths, respectively. As a result, even when the second-order methods

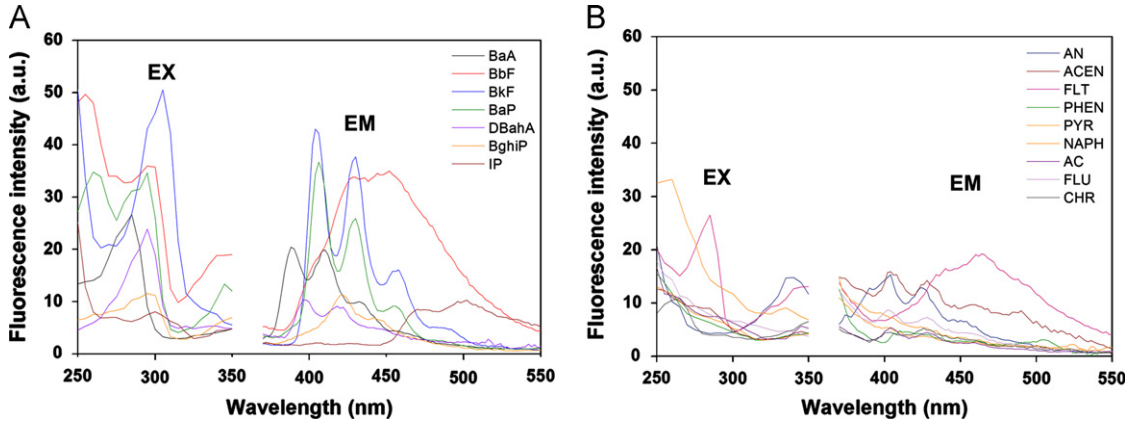

Fig. 1. (A) Excitation (EX) and emission (EM) fluorescence spectra for solutions of 0.50 μg L^{-1} BkF (green) and 2.00 μg L^{-1} of the following: BaP (black), DBahA (red), BbF (blue), BaA (violet), BghiP (magenta), and IP (wine), and (B) for AN (blue), ACEN (wine), FLT (pink), PHEN (olive), PYR (yellow), NAPH (orange), AC (purple), FLU (magenta) and CHR (gray) in *n*-hexane. The λ_{ex} (nm)/λ_{em} (nm) are as follows: 290/410, 270/394, 290/454, 310/406, 290/388, 300/420, and 300/484 for BaP, DBahA, BbF, BkF, BaA, BghiP, and IP, respectively, and 340/402, 255 386, 290/464, 264/390, 320/394, 275/380, 280/380, 280/380, and 275/380 for AN, ACN, FLT, PHEN, PYR, NAPH, AC, FLU, and CHR, respectively. (For interpretation of the references to color in this figure legend, the reader is referred to the web version of this article.)

are used, the sample preparation step is hard to avoid. The proposed sample preparation combining microwave-assisted L–L extraction with SPE on silica permit the analytes to be extracted and eliminates the primary interferences for the clear detection of PAHs in edible oils.

Based on our experiences and in agreement with Moret and Conte [38], no more than 50 mg of oil per gram of silica should be loaded onto the SPE cartridge to avoid fat breakthrough into the PAH fraction. Therefore, due to the amount of co-extracted oil in the proposed extraction process (88 ± 4 mg and 171 ± 9 mg dissolved in 1 mL as the final volume for EVOO and SO, respectively), the volume loaded onto the SPE cartridge was 1 mL for the EVOO samples and 0.5 mL for the SO samples.

4.2. Second-order multivariate calibration

Chemometric analysis with PARAFAC and U-PLS/RBL algorithms were applied to the EEFM data due to the matrix complexity and the overlaps in the PAHs spectra. The best algorithm was defined in the validation step with samples of increasing complexity. First, samples of an organic EVOO that contained the studied analytes were evaluated, and then, samples of different brands and types of edible oils (in this case, four brands of EVOO and two brands of SO) spiked with the same PAHs were studied. Finally, samples of an organic EVOO that contained the nine remaining US-EPA-PAHs were analyzed.

4.2.1. Validation set samples

To construct the second-order calibration models, EEFMs were recorded in a wide spectral range that included the fluorescence signals of all of the analytes studied.

PARAFAC was applied to the three-way data arrays constructed by combining the data matrices for each validation sample with those of the set of calibration samples. The selection of the optimum spectral range and the optimum number of factors was performed using the criterion of similarity (correlation coefficient, r), percentage of fit and the core consistency test [24,26]. In U-PLS/RBL, the selection was performed using the cross-validation method described by Haaland and Thomas [29] over just the calibration set. The optimum number of factors is estimated by calculating the ratio $F(A)=\mathrm{PRESS}(A<A^*)/\mathrm{PRESS}(A)$, where PRESS is the predicted error sum of squares, defined as $\mathrm{PRESS}=\Sigma_1^I\left(y_{\mathrm{nominal}}-y_{\mathrm{predicted}}\right)^2$, A is a trial number of factors and A^* corresponds to the minimum PRESS. The number of optimum factors was selected as that leading to a probability of less than 75% and $F>1$. Note that RBL is not required for calibration samples because they did not include unexpected components.

Table 1
Number of factors (A) and excitation–emission wavelength ranges used in the U-PLS and PARAFAC methods.

	PARAFAC			U-PLS		
	A	Excitation (nm)	Emission (nm)	A	Excitation (nm)	Emission (nm)
BaA	6	260–325	374–444	6	260–325	374–444
BbF	5	300–345	376–500	6	300–345	376–500
BkF	4	260–340	370–470	5	260–340	370–450
BaP	6	270–350	378–482	7	270–350	378–482
DBahA	7	260–340	384–462	8	260–340	384–462
BghiP	8	250–330	370–498	8	250–330	370–498
IP	4	320–380	450–490	4	320–380	450–490

Table 1 presents the number of factors and the final excitation and emission spectral ranges selected for each analyte when PARAFAC and U-PLS were applied. The optimum spectral ranges for each analyte were almost the same. The number of factors estimated for PARAFAC was equal to or less than that for U-PLS. This result is due to the fact that U-PLS provides latent variables (abstract loadings and regression coefficients) that do not have any physical interpretation, and only the adequate fit of the sample signal to the calibration model indicates that the correct analyte is quantified. In contrast, PARAFAC provides physically interpretable profiles, and the identification of the chemical constituents under investigation is performed for comparing the estimated profiles with those for a standard solution of the analyte of interest.

PARAFAC and U-PLS/RBL were then applied to predict the analyte concentration in the validation samples. In this case, RBL is required for the validation samples because they contain unexpected components due to the oil matrix. Fig. 2A and C present three-dimensional plots of the EEFMs for a typical calibration sample and an organic EVOO sample, respectively. The real challenge we are facing is evident when observing these figures and comparing them with Fig. 2B, which shows the EEFM for a typical validation sample that includes the seven studied analytes and the oil matrix. Consequently, when U-PLS/RBL was applied to the validation samples, in addition to the latent variables estimated for each analyte from the calibration set, the introduction of the RBL procedure with an additional number of factors that corresponds to the unexpected oil constituents was required. The number of RBL factors, which were estimated according to the procedure above described [18], ranged from 1 to 4, depending on the analyzed PAH and the corresponding spectral range.

The statistical results for the determination of the seven studied PAHs in the validation samples using PARAFAC and U-PLS/RBL are shown in Table 2. U-PLS/RBL yielded good predictions for PAHs with a relative error (REP) equal to or less than 15%, except in the case of BghiP, which presented a REP of 25%. However, considering the complexity of the system, the latter value can be acceptable. In contrast, a poorer prediction was observed when PARAFAC was applied with REPs greater than 20%, and BghiP and IP were the worst predicted analytes. In fact, PARAFAC could not predict the concentrations of BghiP in the validation samples. This fact may be attributed to the low fluorescence intensity and the significant spectral overlapping of these analytes (BghiP and IP) with the matrix, which prevents the successful decomposition of the second-order data.

In Chile and Spain, the maximum admissible concentration level for eight heavy US-EPA-PAHs in edible oils is 2.0 $\mu g\,kg^{-1}$ for each single PAH, including BaA, BbF, BkF, BaP, BeP, DBahA, BghiP, and IP, and 5.0 $\mu g\,kg^{-1}$ for the total PAH content. The limits of detection (LODs) obtained using U-PLS/RBL were less than 1.0 $\mu g\,kg^{-1}$, except for BghiP and IP (1.8 and 2.0 $\mu g\,kg^{-1}$, respectively). Although the LOD for these analytes are on the order of 2.0 $\mu g\,kg^{-1}$, it can be acceptable for its determination in potentially contaminated samples. Furthermore, the LODs obtained using the U-PLS/RBL method are on the order of those reported for HPLC-FLD methods [2,4,7,9,41]. Although the LODs obtained using PARAFAC were less than 2.0 $\mu g\,kg^{-1}$ for BaA, BbF, BkF and DBahA, they were almost 2 or 3 times greater than those obtained using U-PLS/RBL. The highest LODs were obtained for BaP and IP (4.6 and 4.8 $\mu g\,kg^{-1}$, respectively), and they exceeded the regulatory limit for each single PAH.

The poor results obtained using PARAFAC could be attributed to its inability to model a system where the spectroscopic profiles of the analytes are similar among them as well as with the matrix components. Therefore, only the U-PLS/RBL method was applied for the prediction of PAHs in the edible oil samples.

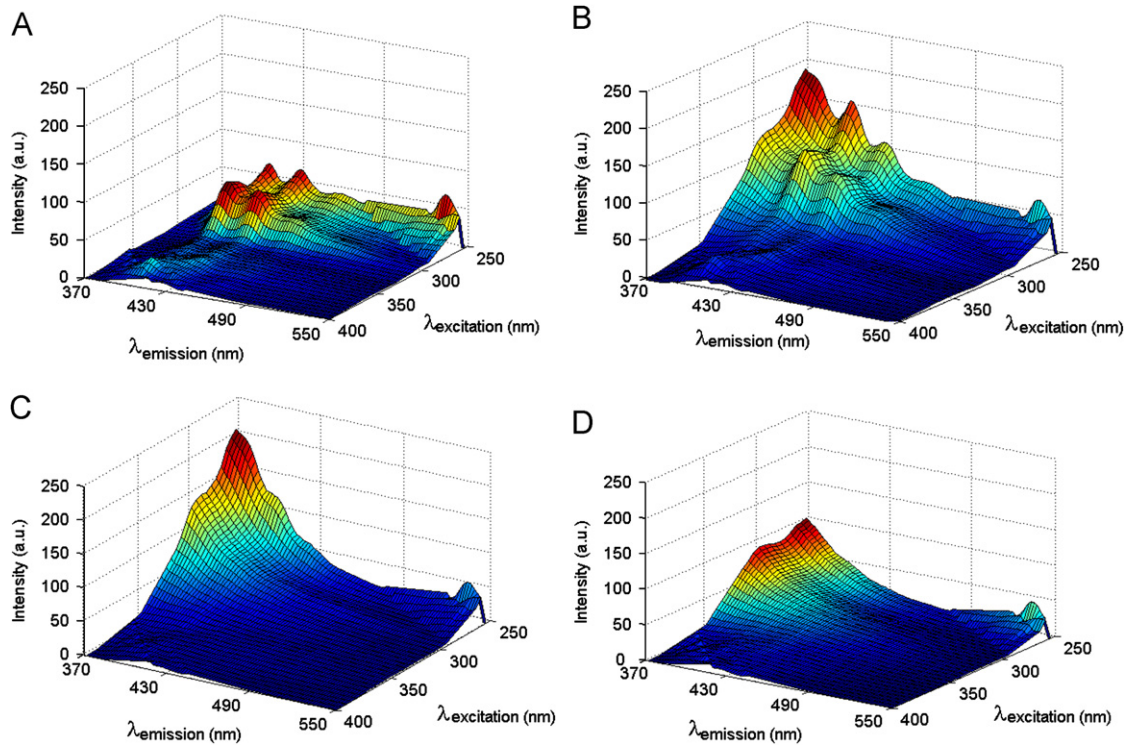

Fig. 2. Three-dimensional plots for the excitation–emission fluorescence matrices corresponding to (A) a calibration sample containing 1.06 μg L^{-1} of BaP, DBahA, BbF, BaA and BghiP, 0.29 μg L^{-1} BkF, and 1.50 μg L^{-1} IP, and (B) a validation sample containing the seven PAHs at the same concentrations of the calibration sample, (C) an organic EVOO sample, and (D) a SO sample.

Table 2
Statistical results for the determination of PAHs in validation samples.

	PARAFAC							U-PLS/RBL						
	BaA	BbF	BkF	BaP	DBahA	BghiP	IP	BaA	BbF	BkF	BaP	DBahA	BghiP	IP
RMSEP (μg kg^{-1})[a]	0.62	1.2	0.25	1.1	0.59	–	3.4	0.24	0.43	0.09	0.35	0.26	0.89	0.52
REP (%)[b]	25	42	37	46	24	–	98	10	15	13	15	11	25	15
γ^{-1} (μg kg^{-1})[c]	0.27	0.34	0.07	1.4	0.38	–	1.5	0.16	0.13	0.02	0.11	0.16	0.54	0.61
LOD (μg kg^{-1})[d]	0.91	1.1	0.24	4.6	1.3	–	4.8	0.51	0.43	0.07	0.35	0.53	1.8	2.0

[a] Root mean square error of prediction, $RMSEP = [(1/I)\sum_1^I (c_{nominal} - c_{predicted})^2]^{1/2}$, where I is the number of prediction samples and $c_{nominal}$ and $c_{predicted}$ are the actual and predicted concentrations, respectively.
[b] Relative error of prediction, $REP = 100 \times RMSPE/c_{mean}$ where c_{mean} is the mean calibration concentration.
[c] Inverse of the analytical sensitivity (γ), $\gamma^{-1} = s_x/SEN_n$ where s_x is the instrumental noise and SEN_n is the sensitivity [39]. The s_x and SEN_n values are averages of the values corresponding to 11 validation samples.
[d] Limit of detection, $LOD = 3.3\ \gamma^{-1}$, Ref. [40].

4.2.2. Test samples of spiked edible oils

The predictive capacity of the calibration model using U-PLS/RBL was evaluated with different brands and types of edible oils. A total of 25 spiked samples of edible oils were analyzed, including 17 samples of four different brands of EVOO and 8 samples of two brands of SO. Fig. 2C and D present the three-dimensional plots of the EEFM for an organic EVOO and an SO sample, respectively. Despite the apparent fluorescence intensity differences between the EVOO and SO samples, their excitation–emission profiles are similar. Consequently, additional RBL factors other than those estimated for the validation samples were not required for the predictions of the analytes with U-PLS/RBL. Table 3 presents the mean recovery and the predictive capacity results obtained for the determination of the seven studied PAHs in these samples.

As can be observed, the mean recoveries obtained using U-PLS/RBL ranged from 64 to 81% and were in agreement with the values previously reported for the sample preparation method employed in this study [37]. On the other hand, no significant differences between the concentrations predicted by U-PLS/RBL and the concentrations obtained from HPLC-FLD were observed (Table 3); consequently, the theoretical (1,0) points are included or are close to the borders of the elliptical joint regions. Fig. 3 presents the plots of the U-PLS/RBL predicted concentrations as a function of the obtained values by HPLC-FLD and the corresponding elliptical joint regions (at a 95% confidence level) for BaA and BaP (as representative compounds of the studied group). In addition, the mean recoveries (in percentage) for the 25 samples were calculated and compared using a paired t-test, and no significant differences between the methods were observed (p-value: 0.80 at 95% confidence). Therefore, based on the obtained results, the proposed method using EEFMs coupled with U-PLS/RBL is comparable with the reference HPLC-FLD method.

Table 3
Part A Recovery and predictive capacity study for seven studied PAHs in spiked samples of different types and brands of edible oil samples using the U-PLS/RBL and HPLC-FLD as reference method.

Oil	Brand	Sample	BaA			BbF			BkF			BaP		
			Nominal (μg kg^{-1})	U-PLS/RBL Predicted (μg kg^{-1})	HPLC-FLD (μg kg^{-1})	Nominal (μg kg^{-1})	U-PLS/RBL Predicted (μg kg^{-1})	HPLC-FLD (μg kg^{-1})	Nominal (μg kg^{-1})	U-PLS/RBL Predicted (μg kg^{-1})	HPLC-FLD (μg kg^{-1})	Nominal (μg kg^{-1})	U-PLS/RBL Predicted (μg kg^{-1})	HPLC-FLD (μg kg^{-1})
EVOO	A	1	5.4	3.1	3.4	4.8	4.2	3.0	1.2	1.0	0.85	4.5	1.7	2.3
		2	0.60	< LOD	0.56	5.7	3.7	3.7	0.60	0.27	0.31	4.8	2.5	2.7
		3	5.4	3.6	3.9	3.9	2.8	2.9	1.2	0.79	0.89	1.2	0.83	0.79
		4	3.9	2.8	3.1	5.1	3.4	3.8	0.30	0.28	0.27	3.0	1.8	2.0
	B	5	0.60	0.87	0.67	5.7	4.2	4.0	0.40	0.38	0.36	2.7	1.8	1.6
		6	1.5	1.7	1.4	3.9	3.4	3.1	1.2	1.3	0.97	3.9	2.9	2.5
		7	3.0	2.5	2.5	4.5	3.4	3.3	0.90	0.80	0.63	4.2	2.9	2.4
		8	5.7	4.1	5.2	2.4	2.0	2.1	0.90	0.70	0.76	4.5	3.1	3.2
	C	9	5.7	4.2	4.8	0.9	1.0	0.80	1.2	0.98	1.1	1.5	0.85	1.3
		10	0.90	0.7	0.76	4.2	2.9	3.0	0.60	0.34	0.45	3.9	2.3	2.6
		11	5.7	4.2	4.5	1.5	1.6	1.3	0.60	0.52	0.53	3.9	2.3	2.6
		12	5.7	4.3	4.3	0.6	0.68	0.59	1.8	1.3	1.4	0.90	0.41	0.68
	D	13	2.7	1.9	2.2	4.8	3.7	3.6	0.2	0.22	0.28	0.60	0.84	0.56
		14	4.8	3.8	3.7	1.8	2.1	1.4	0.9	0.66	0.70	3.0	2.3	2.1
		15	0.90	0.96	1.0	5.7	4.5	4.9	1.5	1.1	1.3	5.7	4.2	4.0
		16	2.4	2.0	2.0	2.4	2.0	2.0	0.3	0.28	0.31	2.1	1.4	1.5
		17	5.4	3.4	3.9	2.1	1.4	1.6	0.6	0.29	0.45	3.6	2.2	2.1
SO	E	18	6.0	3.3	4.6	11	7.5	7.6	2.4	1.5	1.8	9.6	5.8	5.9
		19	11	6.7	7.3	6.0	4.3	3.7	1.8	1.2	1.4	9.0	5.5	5.9
		20	11	6.0	7.4	9.0	6.1	6.2	1.2	0.72	0.90	7.2	4.6	4.5
		21	7.8	5.0	5.6	10	6.1	6.2	0.6	0.42	0.54	6.0	3.4	3.1
	F	22	6.0	7.2	6.7	11	8.4	10	2.4	1.4	1.6	9.6	6.0	7.2
		23	11	7.1	7.8	6.0	4.6	4.8	1.8	1.2	1.7	9.0	5.3	6.1
		24	11	9.5	7.3	9.0	7.1	6.4	1.2	0.93	1.1	7.2	4.7	4.7
		25	7.8	5.4	5.9	10	7.0	7.1	0.6	0.54	0.60	6.0	3.9	4.0
Mean Recovery % (n=25)				78	82		80	76		76	83		65	66

Part B

Oil	Brand	Sample	DBahA			BghiP			IP		
			Nominal (μg kg^{-1})	U-PLS/RBL Predicted (μg kg^{-1})	HPLC-FLD (μg kg^{-1})	Nominal (μg kg^{-1})	U-PLS/RBL Predicted (μg kg^{-1})	HPLC-FLD (μg kg^{-1})	Nominal (μg kg^{-1})	U-PLS/RBL Predicted (μg kg^{-1})	HPLC-FLD (μg kg^{-1})
EVOO	A	1	1.2	0.95	0.75	1.2	< LOD	0.87	2.4	0.8	1.6
		2	4.5	3.0	2.2	7.5	4.3	3.7	5.7	4.0	3.3
		3	1.5	2.1	1.1	5.7	5.4	3.3	2.1	2.5	1.7
		4	3.0	2.5	2.0	4.2	3.0	2.6	3.9	1.9	2.4
	B	5	4.2	3.0	2.6	9.9	4.0	5.6	1.8	< LOD	1.7
		6	5.4	4.4	3.6	6.9	3.6	4.3	4.5	4.2	3.3
		7	5.7	3.0	3.6	6.3	4.0	3.6	1.8	< LOD	1.4
		8	3.0	3.3	2.4	11	6.1	6.3	4.8	4.1	3.8
	C	9	0.90	1.0	0.64	3.3	2.4	2.4	5.1	4.8	3.9
		10	0.90	1.2	0.64	9.0	6.0	5.0	5.7	3.5	3.9
		11	1.5	1.4	1.1	9.0	6.2	5.3	3.3	2.4	2.3
		12	5.1	3.1	3.4	4.5	4.3	2.4	6.9	5.4	4.7
	D	13	1.5	1.4	1.2	6.9	5.0	4.2	6.0	2.8	4.3
		14	4.8	3.6	3.4	0.9	< LOD	0.64	3.9	3.0	2.9
		15	1.2	1.2	1.2	0.6	< LOD	0.65	7.5	5.2	5.3
		16	5.4	3.8	4.0	1.5	< LOD	1.2	2.7	1.2	1.9
		17	2.1	1.4	1.5	6.6	1.9	3.6	7.2	3.2	4.6
SO	E	18	9.0	5.9	5.9	15	8.8	8.9	11	6.8	7.4
		19	6.0	3.2	4.6	22	13	16	13	6.8	8.9

Table 3 (*continued*)

Part B												
Oil	Brand	Sample	DBahA			BghiP			IP			
			Nominal ($\mu g\ kg^{-1}$)	U-PLS/RBL Predicted ($\mu g\ kg^{-1}$)	HPLC-FLD ($\mu g\ kg^{-1}$)	Nominal ($\mu g\ kg^{-1}$)	U-PLS/RBL Predicted ($\mu g\ kg^{-1}$)	HPLC-FLD ($\mu g\ kg^{-1}$)	Nominal ($\mu g\ kg^{-1}$)	U-PLS/RBL Predicted ($\mu g\ kg^{-1}$)	HPLC-FLD ($\mu g\ kg^{-1}$)	
		20	7.8	4.7	5.5	17	9.4	11	14	8.2	9.5	
		21	7.2	4.4	4.9	23	12	13	12	5.5	7.7	
	F	22	9.0	6.6	7.0	15	11	13	11	6.5	11	
		23	6.0	5.8	4.9	22	13	15	13	8.6	9.4	
		24	7.8	5.2	5.5	17	13	11	14	8.3	9.4	
		25	7.2	5.1	5.3	23	12	15	12	5.7	8.3	
Mean Recovery % ($n=25$)				81	71		64	65		66	71	

4.2.3. Test samples containing unexpected PAHs

For evaluating the capacity of U-PLS/RBL to resolve the seven PAHs selected in the presence of the remaining nine US-EPA-PAHs priority pollutants, four samples of organic EVOO spiked with both groups of PAHs were processed. As stated above, for the U-PLS/RBL method, no additional RBL factors other than those used for the validation samples were required for the interferences. This result could be attributed to the fact that these PAHs have fluorescence profiles that do not significantly overlap with those of the studied compounds. Table 4 presents the prediction results that correspond to the application of U-PLS/RBL and the values obtained by HPLC-FLD. The comparison between the methods was performed for each PAH by applying a mean-*t* test to the set of evaluated organic EVOO samples at a 98% significance level [42]. No significant differences were observed for any of the studied PAHs, which suggests that the values for each PAH concentration obtained by applying the UPLS-RBL method are statistically comparable with those provided by the reference HPLC-FLD technique. Furthermore, these results suggest that the remaining nine US-EPA-PAHs that may be present in the edible oils do not produce a significant interference in the proposed analysis.

4.2.4. Precision of the proposed method

A within-day ($n=4$) and between-day ($n=4$) precision study was performed by processing an organic EVOO sample spiked with the seven PAHs. The results are provided in Table 5. The relative standard deviation for the intra-day precision was equal to or less than 8%, whereas the between-day precision was equal to or less than 13%. The principal source of error is related to the irreproducibility of the sorbent material in the cartridges of silica used during the SPE. However, these values are sufficiently satisfactory, considering the complexity of the matrix and the low concentration level of the analytes.

4.2.5. Real samples

A set of twenty samples of edible oils (five brands of SO, one SO used to prepare fried fish and fourteen brands of EVOO) were analyzed using the proposed method and using HPLC-FLD. None of the samples of SO exhibited PAHs at detectable concentrations. However, only in three EVOO samples (21%), one of the seven tested PAHs was detected (BkF). These samples had 0.09; 0.18 and 0.24 $\mu g\ kg^{-1}$ of BkF. The results obtained using HPLC-FLD were similar compared to those obtained using UPLS-RBL (0.15; 0.21 and 0.18 $\mu g\ kg^{-1}$, respectively).

5. Conclusions

Fluorescence excitation–emission matrices associated with U-PLS/RBL have been demonstrated to be a powerful tool for resolving a mixture of heavy US-EPA-PAHs in the presence of a very complex matrix such as that of edible oil. Although the method can resolve the mixture of analytes in the presence of unexpected compounds, the complexity of the matrix with native compounds that presents spectral overlapping with the PAHs, as well as being able to produce inner filter effects in particular, necessitate a sample treatment procedure for a selective detection of PAHs. Therefore, the combination of microwave-assisted L–L extraction with SPE on silica permitted the analytes to be extracted and eliminated the interferences. The strength of the proposed method was tested by predicting the selected PAHs in different brands and types of edible oils and in the presence of the remaining US-EPA-PAHs priority pollutants. The U-PLS/RBL predicted concentrations were compared with the values obtained using HPLC-FLD, and no significant differences between them

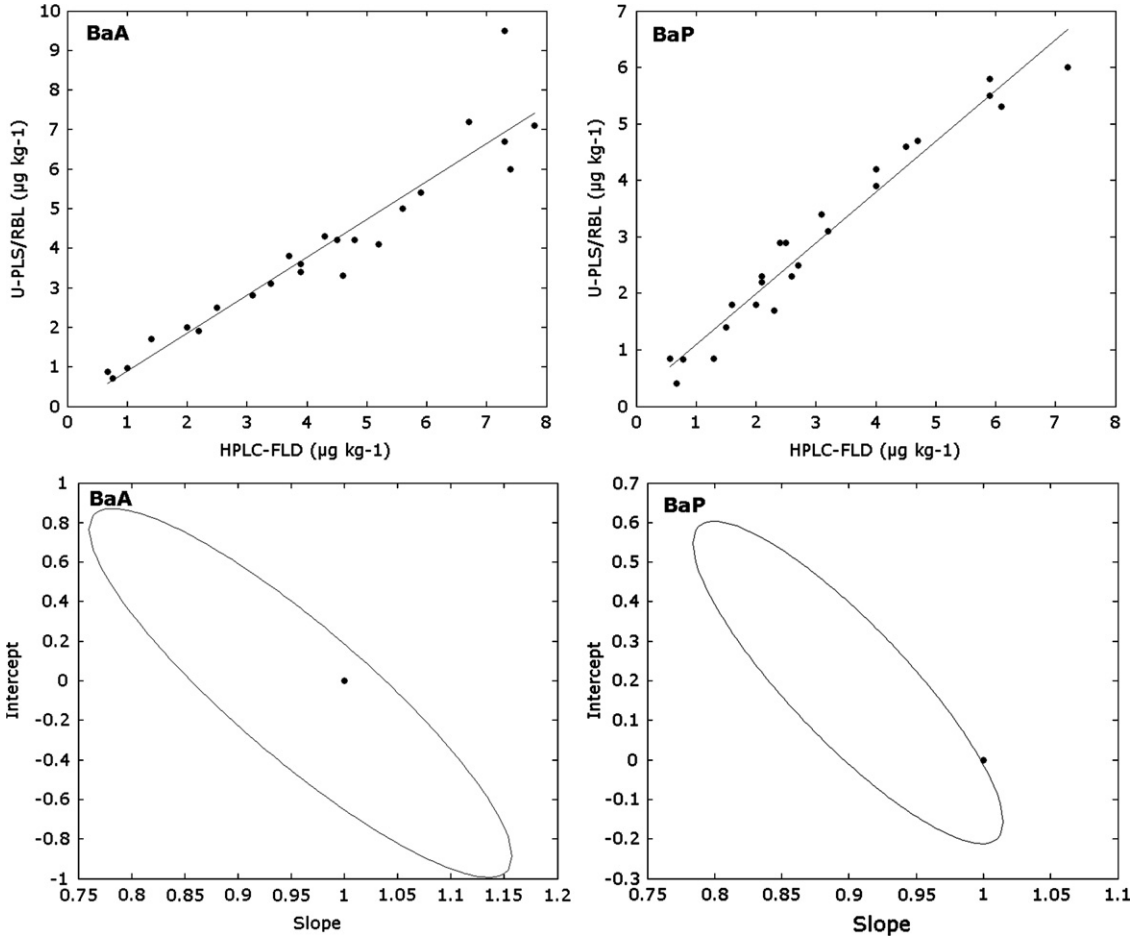

Fig. 3. Plots for U-PLS predicted concentrations as a function of the obtained HPLC-FLD values for BaA and BaP and the corresponding elliptical joint regions (at 95% confidence level) for the slopes and intercepts of the regression for the U-PLS/RBL versus HPLC-FLD plots. The black circle in the elliptical plots marks the theoretical point (intercept: 0, slope: 1).

Table 4
Part A Determination of the seven studied PAHs concentrations in the presence of the remaining nine US-EPA-PAHs priority pollutants[a] in spiked organic EVOO samples using UPLS/RBL and HPLC-FLD as a reference method.

	BaA			BbF			BkF			BaP		
	U-PLS/RBL ($\mu g\ kg^{-1}$)	HPLC-FLD ($\mu g\ kg^{-1}$)	t^b	U-PLS/RBL ($\mu g\ kg^{-1}$)	HPLC-FLD ($\mu g\ kg^{-1}$)	t^b	U-PLS/RBL ($\mu g\ kg^{-1}$)	HPLC-FLD ($\mu g\ kg^{-1}$)	t^b	UPLS-RBL ($\mu g\ kg^{-1}$)	HPLC-FLD ($\mu g\ kg^{-1}$)	t^b
Sample 1	3.0	3.2		2.9	2.6		1.5	1.5		2.4	2.2	
Sample 2	3.8	3.5		3.3	3.0		1.6	1.7		2.6	2.6	
Sample 3	2.8	3.5		3.3	2.8		1.9	1.7		2.9	2.5	
Sample 4	2.5	3.5		3.3	2.9		1.8	1.7		2.6	2.6	
Mean concentration ($n=4$)	3.0	3.4	1.39	3.2	2.8	2.85	1.7	1.7	0.48	2.6	2.5	1.07

Part B

	DBahA			BghiP			IP		
	U-PLS/RBL ($\mu g\ kg^{-1}$)	HPLC-FLD ($\mu g\ kg^{-1}$)	t^b	U-PLS/RBL ($\mu g\ kg^{-1}$)	HPLC-FLD ($\mu g\ kg^{-1}$)	t^b	U-PLS/RBL ($\mu g\ kg^{-1}$)	HPLC-FLD ($\mu g\ kg^{-1}$)	t^b
Sample 1	2.7	2.6		2.9	2.8		3.4	3.5	
Sample 2	2.5	2.9		2.9	3.3		3.9	3.8	
Sample 3	3.1	2.8		2.7	3.2		5.4	3.8	
Sample 4	2.8	2.8		1.7	3.3		4.7	4.0	
Mean concentration ($n=4$)	2.8	2.8	0.00	2.6	3.2	1.93	4.4	3.8	1.27

[a] Concentration of the remaining nine US-EPA-PAHs = 3 $\mu g\ kg^{-1}$.
[b] Calculated student t statistic for a mean t test. The critical t value for (n_1+n_2-2) degrees of freedom and at the 98% significance level is $t_{crit(0.02,2)}=3.14$ [42].

Table 5
Within-day ($n=4$) and between-day ($n=4$) precision of spiked organic EVOO samples using UPLS/RBL.

	Added ($\mu g\ kg^{-1}$)	Within-day precision		Between-day precision	
		SD	RSD	SD	RSD
BaA	3	0.23	8	0.09	3
BbF	3	0.15	7	0.25	13
BkF	0.75	0.02	4	0.05	8
BaP	3	0.20	8	0.29	11
DBahA	3	0.14	5	0.27	11
BghiP	6	0.45	7	0.65	11
IP	6	0.38	6	0.55	9

were observed. Additionally, note that the LODs obtained using the proposed method are still comparable to those reported using HPLC methods. Therefore, the proposed method using EEFMs coupled with U-PLS/RBL are comparable and provide a suitable alternative to the chromatographic method.

Acknowledgments

The authors gratefully acknowledge the financial support of Fondecyt (project 1110114). Francis Alarcón also thanks CONICYT for the doctoral grant and the award in support of his thesis development.

References

[1] R. Simon, J.A.G. Ruiz, C. VonHolst, T. Wenzl, E. Anklam, Anal. Bioanal. Chem. 391 (2008) 1397–1408.
[2] S. Martínez, A. Morales, A. Pastor, A. Morales, M. Guardia, J. AOAC Int. 88 (2005) 1247–1254.
[3] S. Moret, L.S. Conte, J. Sep. Sci. 25 (2002) 96–100.
[4] V.H. Teixeira, S. Casal, M.B. Oliveira, Food Chem. 104 (2007) 106–112.
[5] F.J. Arrebola, A.G. Frenich, M.J.G. Rodríguez, P.P. Bolaños, J.L.M. Vidal, J. Mass Spectrom. 41 (2006) 822–829.
[6] G. Diletti, G. Scortichini, R. Scarpone, G. Gatti, L. Torreti, G. Migliorati, J. Chromatogr. A 1062 (2005) 247–254.
[7] A. Barranco, R.M.A. Salces, A. Bakkali, L.A. Berrueta, B. Gallo, F. Vicente, M. Sarobe, J. Chromatogr. A 988 (2003) 33–40.
[8] M. Guillén, P. Sopelana, G. Palencia, J. Agric. Food Chem. 52 (2004) 2123–2132.
[9] M.A. Lage, J.L. Cortizo, Food Control 16 (2005) 59–64.
[10] S. Moret, G. Purcaro, L.S. Conte, Eur. J. Lipid Sci. Technol. 107 (2005) 488–496.
[11] G. Purcaro, S. Moret, L.S. Conte, J. Sep. Sci. 31 (2008) 3936–3944.
[12] Boletín Oficial del Estado (España). Límites de Determinados Hidrocarburos Aromáticos Policíclicos en Aceite de Orujo de Oliva. N° 178 (2001) 27398. Orden de 25 de julio de 2001, Madrid, Spain.
[13] Ministerio de Salud Republica de Chile. Reglamento Sanitario de los Alimentos DTO N°977/96 Modificación Dto 115/03 Minsal, Articulo 249 (2009) 97–98, Santiago, Chile.
[14] K.S. Booksh, A.R. Muroski, M.L. Myrick, Anal. Chem. 68 (1996) 3539–3544.
[15] E. Sikorska, T. Górecki, I.V. Khmelinskii, M. Sikorski, J. Koziol, Food Chem. 89 (2005) 217–225.
[16] G.M. Escandar, N.M. Faber, H.C. Goicochea, A. Muñoz de la Peña, A.C. Olivieri, R.J. Poppi, Trends Anal. Chem. 26 (2007) 752–765.
[17] A.C. Olivieri, Anal. Chem. 80 (2008) 5713–5720.
[18] S.A. Bortolato, J.A. Arancibia, G.M. Escandar, Anal. Chem. 80 (2008) 8276–8286.
[19] S.A. Bortolato, J.A. Arancibia, G.M. Escandar, Environ. Sci. Technol. 45 (2011) 1513–1520.
[20] S. Yu, H.C. Goicoechea, A.D. Campiglia, Appl. Spectrosc. 61 (2007) 165–170.
[21] H.Y. Wang, S.J. Yu, A.D. Campiglia, Anal. Biochem. 385 (2009) 249–256.
[22] W.B. Wilson, A.D. Campiglia, Analyst 136 (2011) 3366–3374.
[23] J. Christensen, L. Nørgaard, R. Bro, S.B. Engelsen, Chem. Rev. 106 (2006) 1979–1994.
[24] R. Bro, Chemom. Intell. Lab. Syst. 38 (1997) 149–171.
[25] K.S. Booksh, A.R. Muroski, M.L. Myrick, Anal. Chem. 68 (1996) 3539–3544.
[26] R. Bro, H.L.A. Kiers, J. Chemom. 17 (2003) 274–286.
[27] S. Wold, P. Geladi, K. Esbensen, J. Öhman, J. Chemom. 1 (1987) 41–56.
[28] A.C. Olivieri, J. Chemom. 19 (2005) 253–265.
[29] D.M. Haaland, E.V. Thomas, Anal. Chem. 60 (1988) 1193–1202.
[30] J. Öhman, P. Geladi, S. Wold, J. Chemom. 4 (1990) 135–146.
[31] R.G. Zepp, W.M. Sheldon, M.A. Moran, Mar. Chem. 89 (2004) 15–36.
[32] MATLAB 6.0, The MathWorks Inc., Natick, MA, USA, 2000.
[33] 〈http://www.models.kvl.dk/algorithms〉 (Last visit on July 26, 2012).
[34] A.C. Olivieri, H.L. Wu, R.Q. Yu, Chemom. Intell. Lab. Syst. 96 (2009) 246–251.
[35] Chemometry Consultancy, 〈http://www.chemometry.com〉 (Last visit on July 26, 2012).
[36] E. Fuentes, M.E. Báez, J. Díaz, J. Chromatogr. A 1216 (2009) 8859–8866.
[37] F. Alarcón, M.E. Báez, M. Bravo, P. Richter, E. Fuentes, Talanta (2012).
[38] S. Moret, L.S. Conte, J. Sep. Sci. 25 (2002) 96–100.
[39] A.C. Olivieri, N.M. Faber, J. Chemom. 19 (2005) 583–592.
[40] R. Boque, M.S. Larrechi, F.X. Rius, Chemom. Intell. Lab. Syst. 45 (1999) 397–408.
[41] R. Weißhaar, Eur. J. Lipid Sci. Technol. 104 (2002) 282–285.
[42] J.N. Miller, J.C. Miller, Statistic and Chemometrics for Analytical Chemistry, fourth ed., Pearson Education S.A., Madrid, Spain, 2002, p. 263.